Wood waste-based functionalized natural hydrochar for the effective removal of Ce(III) ions from aqueous solution

Glaydson S. dos Reis[1], Carlos E. Schnorr[2], Guilherme L. Dotto[3,4*], Julien Vieillard[4], Matias S. Netto[3], Luis F. O. Silva[2], Irineu A. S. De Brum[5], Mikael Thyrel[1], Éder C. Lima[5], Ulla Lassi[6,7]

[1-]Department of Forest Biomaterials and Technology, Biomass Technology Centre, Swedish University of Agricultural Sciences, Umeå SE-901 83, Sweden.

[2-]Universidad De La Costa, Calle 58 # 55–66, 080002 Barranquilla, Atlántico, Colombia.

[3-]Research Group on Adsorptive and Catalytic Process Engineering (ENGEPAC), Federal University of Santa Maria, Av. Roraima, 1000-7, 97105–900 Santa Maria, RS, Brazil.

[4-]Normandie Université, UNIROUEN, INSA Rouen, CNRS, COBRA (UMR 6014), 27000 Evreux, France.

[5-]Institute of Chemistry, Federal University of Rio Grande do Sul, 91501-970, P.O.15003, Porto Alegre, Brazil.

[6-]Research Unit of Sustainable Chemistry, University of Oulu, P.O. Box 3000, FI-90014, Oulu, Finland.

[7-]Unit of Applied Chemistry, University of Jyvaskyla, Kokkola University Consortium Chydenius, Talonpojankatu 2B, FI-67100, Kokkola, Finland.

*Corresponding author: Email: guilherme_dotto@yahoo.com.br

Abstract In this study, a sustainable and easily prepared hydrochar from wood waste was studied to adsorb and recover the rare earth element cerium (Ce(III)) from an aqueous

solution. The results revealed that the hydrochar contains several surface functional groups (e.g., C–O, C=O, OH, COOH), which largely influenced its adsorption capacity. The effect of pH strongly influenced the Ce(III) removal, achieving its maximum removal efficiency at pH 6.0 and very low adsorption capacity under an acidic solution. The hydrochar proved to be highly efficient in Ce(III) adsorption reaching a maximum adsorption capacity of 327.9 mg g^{-1} at 298 K. The kinetic and equilibrium process were better fitted by the General order and Liu isotherm model, respectively. Possible mechanisms of Ce(III) adsorption on the hydrochar structure could be explained by electrostatic interactions and chelation between surface functional groups and the Ce(III). Furthermore, the hydrochar exhibited an excellent regeneration capacity upon using 1 mol L^{-1} of sulfuric acid (H_2SO_4) as eluent, and it was reused for three cycles without losing its adsorption performance. This research proposes a sustainable approach for developing an efficient adsorbent with excellent physicochemical and adsorption properties for Ce(III) removal.

Keywords Wood waste; Hydrochar; Sustainable material; Rare earth element; Cerium; Adsorption; Recovery.

Introduction

Waste management and water pollution are serious issues that most affect the environment and the living; therefore, proper management is mandatory to pursue improved life indicators (Bhatnagar et al. 2014). Human activities intrinsically generate vast amounts of waste, especially bio-based wastes, and many of these wastes are not properly managed, which provokes serious environmental contamination and

considerable economic losses (Taelman et al. 2018). However, while biomass waste can be a source of pollution, it can also be a valuable renewable resource for many applications, for example, energy production and materials synthesis (dos Reis et al. 2021a; dos Reis et al. 2021b). Over the last few decades, biomass waste has been successfully employed as precursors for functional bio-based materials synthesis because of their intrinsic structure, abundance, wide availability worldwide, and low cost (dos Reis et al. 2022a; Georgin et al. 2020; Georgin et al. 2019). Due to its rich and various architectures, biomass-advanced carbon materials have evolved into several functional carbons, such as activated carbons and biochars, carbon fibers and gels, and hydrochars (Jiang et al. 2018; Netto et al. 2022).

Hydrochars are produced by hydrothermal carbonization (HTC), a heating method that converts wet biomass at a temperature range of 180–220 °C under subcritical water in saturated pressure conditions (Lima et al. 2022; Azzaz et al. 2020). HTC is a promising method for treating organic wet waste to turn them into functional hydrochar materials (Lima et al. 2022; Netto et al. 2022). However, the successful employment of HTC to produce hydrochars depend on some process factors, including solid/liquid temperatures, holding time, the ratio of water/biomass, and pH of the system biomass/water/solution, where temperature and time have shown to be the most significant factors (Lima et al. 2022; Azzaz et al. 2020; Wang et al. 2018). For example, higher temperatures produced lower solid yields with a higher proportion of gaseous compounds (Yan et al. 2018; Wang et al. 2018), while the residence time plays a huge influence in the distribution and quality of solid, liquid, and gaseous products (Wang et al. 2018).

Hydrochars have been widely employed as an efficient material for amendment and improving polluted soils (Wang et al. 2018). However, in recent years, numerous

works have used hydrochars as bio-adsorbents to remove organic and inorganic compounds through adsorption processes (Kabir et al., 2022a; Kabir et al., 2022b; Kabir et al., 2021; Kabir et al., 2019), mainly due to the large presence of surface functional groups (e.g., COOH, OH, C-O, C=O, etc.) which are responsible for binding pollutants including ions such rare earth elements (REEs), through the electrostatic attraction, ion exchange, and surface complexation (Netto et al. 2022; Xiao et al. 2020; Azzaz et al. 2020).

REEs are essential elements to modern industries, including semi- and superconductors, lasers, fiber optics, batteries, catalysts, etc., and due to their wide range of applications, large amounts of REEs wastes, solids, and liquids are generated (Balaram 2019; Fernandez 2017). Especially the mining of REEs can result in large amounts of tailing, and using elution chemical reagents generates wastewater rich in REEs (Balaram 2019; Fernandez 2017). Thus, it is imperative to treat wastewater containing REEs and recover it for later applications (dos Reis et al. 2022b). Many methods exist to treat and recover REEs from mining and industrial wastewater. However, many face serious drawbacks, such as high energy and chemical consumption and increasing operational costs. However, adsorption appears suitable because of its high effectiveness, easy operation, and low cost (dos Reis et al. 2022b; Azzaz et al. 2020).

Since efficient and cost-effective strategies are required for the future industrial applications of developed sorbents, they allow the building of sustainable adsorbent materials with enhanced microstructural, morphological, and adsorptive properties. Using a sustainable wood waste alternative precursor and an easy and low-cost synthesis approach to increase the share of sustainable raw materials in adsorbent production. This study presents the preparation of a highly efficient hydrochar adsorbent using a sustainable and abundant precursor for removing Ce(III) from an aqueous solution. Very

few reports have dealt with hydrochar for REEs uptake, which further justifies this work. This work aims to produce an eco-friendly and efficient hydrochar to recover an REE (Ce(III)) from synthetic effluents. The physicochemical properties of the hydrochar are thoroughly investigated and correlated to its ability to treat and recover Ce(III) from an aqueous solution. In practice, the idea is to develop a sustainable and green strategy to produce high-performance biomass adsorbent materials to remove REEs from real wastewater.

Materials and methods

Preparation and characterization of the wood waste-based hydrochar (WWH)

The hydrochar was prepared using Prunus serrulata bark as a biomass precursor. The residues were collected on a farm in the region of Santa Maria in Rio Grande do Sul, located in the south of Brazil. The biomass was dried at 105 °C until constant weight and ground using a knife mill machine at particle size under 60 mesh (250 μm). Afterward, 20 grams of milled biomass was mixed in a 100 mL sulfuric acid solution (40%wt.) and stirred for 1.5 hours. Next, the mixture was inserted into a stainless-steel autoclave, internally coated with polypropylene, which was sealed and then treated at 200 °C for six hours. The slurry was then centrifugated to separate solid/liquid fractions from obtaining the hydrochar. After centrifugation, the solid part was dried at 60 °C for 48 h and repeatedly washed until stable pH (around 6).

For the physicochemical characterization of the hydrochar, it was subjected to N_2 adsorption-desorption isotherms, point of zero charges, Fourier-transform infrared spectroscopy (FTIR), X-ray diffraction (XRD), and scanning electron microscopy (SEM).

These characterizations were carried out according to the early works of the ENGEPAC group (Netto et al. 2022; Georgin et al. 2020; Georgin et al. 2019).

Adsorption experiments for Ce(III) uptake

A stock solution of 1000.0 mg L^{-1} of Ce(III) (from Cerium(III) nitrate hexahydrate, Merck) was prepared and diluted to working solutions (0–500 mg L^{-1}) for the adsorption tests. 20 mg of hydrochar was placed in 50 mL Falcon tubes with 20 mL of Ce(III) and agitated at different times (0–240 min). The effect of the initial pH solution on Ce(III) was also evaluated from initial pH varying from 1.0 to 7.0. The effect of the temperature (298 K–328K) on Ce(III) was also evaluated. The tubes were agitated at 200 rpm, and after respective kinetic and equilibrium times, the hydrochar loaded with Ce(III) was separated from the remaining liquid by centrifugation (4000 rpm for 5 min). The concentration of solutions with residual Ce(III) was then subjected to inductively coupled plasma optical emission spectrometry (ICP–OES) (Perkin-Elmer, Waltham, MA, United States) for quantification. The adsorptive performance of the hydrochar was evaluated in terms of the amount of Ce(III) adsorbed per g of adsorbent (q, mg g^{-1}) (Supplementary material). All experiments were duplicated, and blank tests were conducted to check for deviations.

Kinetic, equilibrium, and thermodynamics of Ce(III) adsorption on WWH

The kinetic adsorption data were evaluated using pseudo-first-order (PFO), pseudo-second-order (PSO), and General order models (Guy et al. 2022; Cimirro et al. 2022; Cunha et al. 2020). The isotherms were explored using the nonlinear isotherm models of Freundlich, Langmuir, and Liu (Cimirro et al., 2022; Cunha et al., 2020). The Van't Hoff approach was used to find the adsorption thermodynamic parameters. In this case, the

equilibrium constant was obtained from the best equilibrium constant found in the isotherms from 298-328 K (dos Reis et al. 2022b; Yamil et al. 2020). Details of these models are given in the Supplementary material.

Desorption and regeneration tests

The WWH regeneration was tested in consecutive adsorption-desorption cycles as follows: Firstly, Ce(III) (500 mg L^{-1}) was adsorbed in 1 g L^{-1} WWH solution at 298 K, pH of 6, 250 rpm for 6 h. This experiment led to an adsorption capacity of 312 mg g^{-1}. Then, desorption was performed using 3 g of the Ce(III) loaded WWH, inserted in 100 mL of H_2SO_4 solution, and stirred for 1 h at 300 rpm. The effect of H_2SO_4 concentration was tested from 0.1 to 5 mol L^{-1}. These adsorption-desorption cycles were performed 6 times.

Application in real wastewater

The real wastewater used in this work was a leached liquor of PG (phosphogypsum). The liquor contains Ce (195.0 mg L^{-1}), Dy (3.0 mg L^{-1}), Er (0.8 mg L^{-1}), Eu (2.0 mg L^{-1}), Gd (7.0 mg L^{-1}), La (86.0 mg L^{-1}), Nd (99.0 mg L^{-1}), Pr (18.0 mg L^{-1}), Sm (12.5 mg L^{-1}) and Y (8.5 mg L^{-1}) diluted in citric acid. The liquor also contains phosphates, carbonates, calcium, and iron (Lütke et al., 2022). The adsorption tests in the PG liquor were performed using hydrochar dosages from 1 to 8 g L^{-1}, 200 rpm for 240 min at 298 K. REEs quantification was performed by inductively coupled plasma optical emission spectrometry (ICP–OES) (Lütke et al., 2022).

Results and Discussion

WWH characteristics

The surface morphological structure of the hydrochar was obtained by the SEM (see Fig. 1). The surface of the hydrochar seems to have a high degree of roughness and a very irregular surface. No apparent cavities or holes were observed, suggesting a low porosity degree. The SSA values corroborate this statement. The surface area and pore volume of the hydrochar were measured with 8.8 $m^2\ g^{-1}$ and 0.003 $cm^3\ g^{-1}$, respectively. These values follow what is reported in the literature. For instance, Khoshbouy et al. (2019) prepared hydrochar with an SSA value was 6.3 $m^2\ g^{-1}$. Feng et al. (2019) produced several hydrochars based on food wastes, and their SSA values ranged from 0.25 to 4.75 $m^2\ g^{-1}$. In another work, Li et al. (2022) used bamboo as feedstock to produce hydrochar, and its SSA and pore volume were 2.2699 $m^2\ g^{-1}$ and 0.006424 $cm^3\ g^{-1}$, respectively. Therefore, the hydrochar presented herein has slightly higher SSA values than some reports in the literature. SSA is an important parameter that may boost the adsorption capacities of the adsorbents.

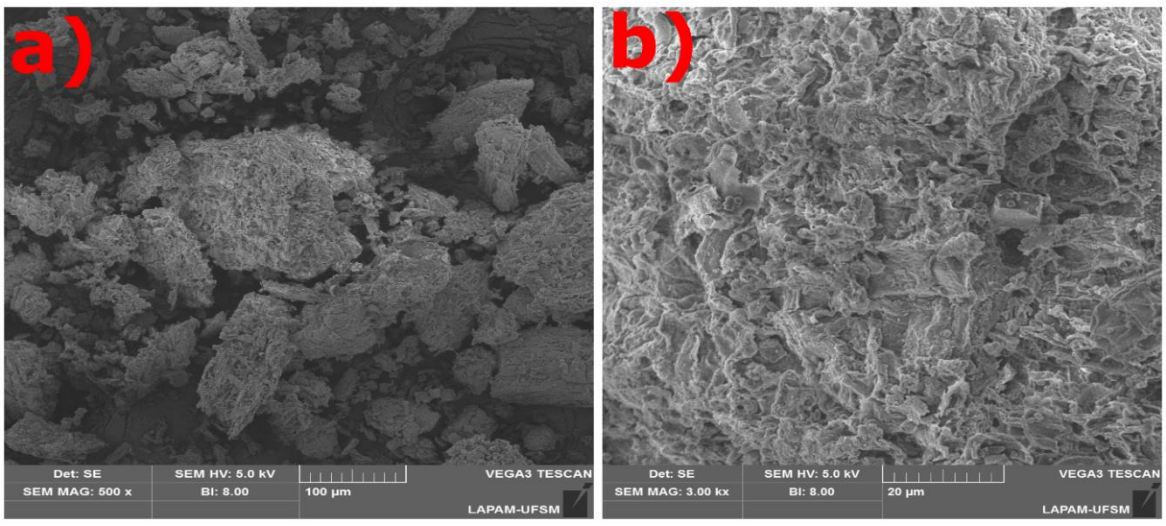

Fig. 1. SEM images of hydrochar at different magnifications.

Still, the SSA value is low compared to other bio-based adsorbents (such as activated carbons and biochars). However, the surface of hydrochar contains many surface functional groups responsible for boosting its adsorption capacity, especially for

194 removing rare earth elements like cerium through electrostatic attraction, ion exchange,
195 and surface complexation.

196 FTIR was performed to examine the surface properties of the hydrochar adsorbent
197 (see Fig. 2a). The spectrum shows that oxygen-containing groups were observed on the
198 hydrochar's surface, which is one of the most important factors affecting the adsorption
199 capacity of REEs (Gonzalez-Hourcade et al. 2022; Li et al. 2022). The FTIR spectrum of
200 hydrochar displayed signals corresponding to; aliphatic C-, aromatic C=O, alkane group,
201 and –OH. Firstly, the bands at 3445 cm^{-1} were attributed to O-H vibrations of hydroxyl
202 groups from adsorbed water molecules. Besides, the band at 1743 cm^{-1} possibly belongs
203 to C=O bonds from ester groups. In addition, the signal at 1617 cm^{-1} is related to the
204 aromatic C=C bond in the hydrochar structure. The bands at around 1050 cm^{-1} could be
205 related to stretching vibrations of C-H, C-O, and C-C-O stretching vibration of cellulose,
206 hemicellulose, and lignin moieties (Netto et al., 2022; Li et al., 2022). A band at 776 cm^{-1}
207 was also observed, corresponding to the aromatic C–H out-of-plane deformation (Li et
208 al., 2022).

209 The XRD pattern of hydrochar, obtained in the 2θ range of 5 to 85° is shown in
210 Fig. 2b. The sharp peak around 20° indicates a crystalline region of cellulose (Keiluweit
211 et al. 2010), which suggests that the HTC treatment was not enough to disrupt crystalline
212 cellulose.

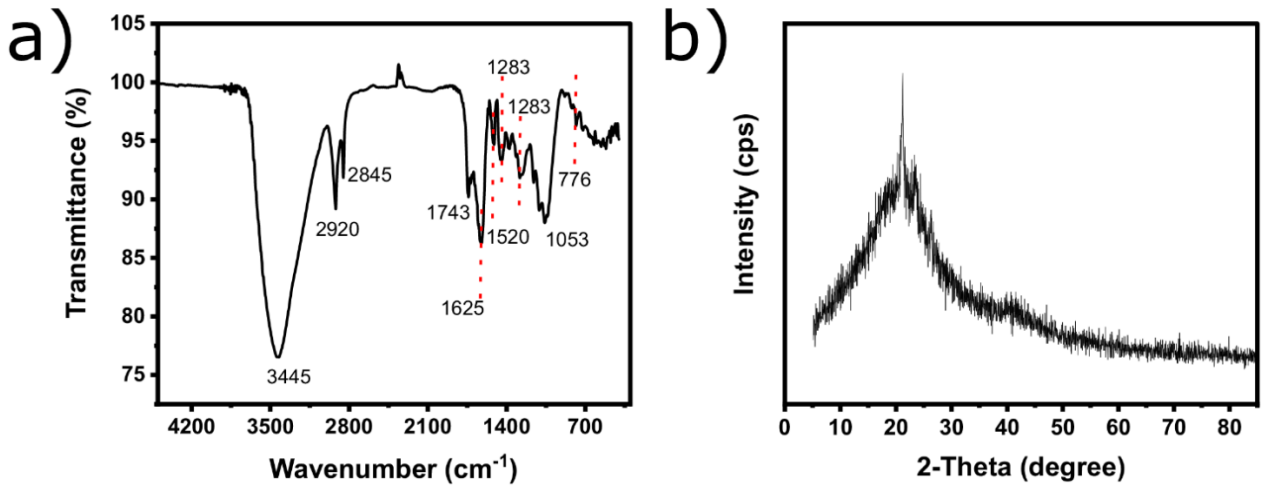

Fig. 2. FTIR a) and XRD pattern b) of hydrochar.

Zeta potential (pH_{pzc}) and pH effect on Ce(III) removal

The pH_{pzc} of the hydrochar was assessed, indicating the point where the hydrochar's surface potential equals zero, which also indicates that values under pH_{pzc} the hydrochar surface charge is positive and above is negative (Lima et al. 2022; dos Reis et al. 2022b). In the case of WWH, a value of 5.1 was found. Therefore, the hydrochar's surface is neutral at pH 5.1. Therefore, at pH values higher than 5.1, the positively charged Ce(III) is easily attracted to the negatively charged hydrochar by a strong electrostatic attraction or chelation (Lima et al. 2022; dos Reis et al. 2022b). Thus, the electrostatic attraction or chelation should be the main mechanism of Ce(III) adsorption.

The pH of a solution is one of the most important parameters affecting the adsorption capacity and equilibrium in wastewater treatment (Lima et al. 2022; dos Reis et al. 2022b) because it not only controls the speciation o pollutants such as rare earth (Ce(III)) but also affect the adsorbent's surface charge. The pH of the Ce(III) solution varied from 1 to 7, and the results are shown in Fig. 3. The results show that the adsorption capacity of the hydrochar was strongly affected by the pH solution as it increased with increasing pH. For example, at pH 1, only 15.7 % was removed; at pH 2, the removal

increased to 25.8%. At pHs 3, 4, 5, and 6, the percentage removals were 48.5%, 54.4%, 77.1%, and 98.6%, respectively, and finally constant at pH 7 (98.6%). This trend suggests that the Ce(III) removal was strongly affected by electrostatic interactions since pH strongly influenced it. The low adsorption capacity of REEs at lower pHs can be caused by the protonation of carboxyl groups, which may act as repulsing the Ce ions. Adversely, with increasing pH, the adsorption capacity improved due to increased surface electronegativity that favors and enhances Ce(III) uptake by the hydrochar's surface through electrostatic attraction.

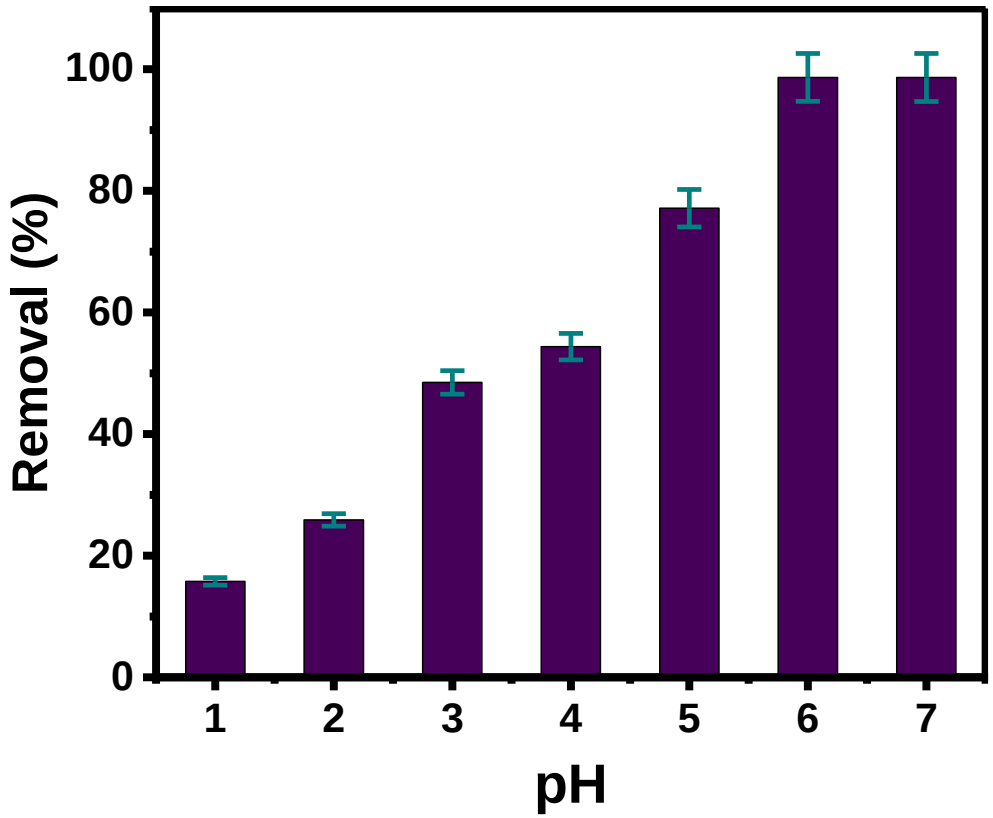

Fig. 3. Effect of pH on Ce(III) removal onto hydrochar.

Kinetic study of Ce(III) onto hydrochar

The kinetic of adsorption is an important step to elucidate the adsorption mechanism of the adsorbate binding process and to understand the rate-controlling adsorption steps

involved in the solid-liquid interaction. The kinetic data of Ce(III) uptake on hydrochar adsorbent was presented in Fig. 4, and the kinetic parameters are shown in Table 1.

R^2_{adj} and SD values were assessed to evaluate the suitability of the kinetic models. The best kinetic fitted model must give the highest R^2_{adj} and lowest SD values. Lower *SD* and higher R^2_{Adj} values suggest a smaller disparity between experimental and theoretical *q* values (Guy et al. 2022; dos Reis et al. 2022c; Lima et al. 2022b). The experimental data seems to follow the General order. By studying the R^2_{adj} and *SD* values in Table 1, they indicate that General order was the most appropriate model to describe the experimental data. Applying the General order model suggests that Ce(III) adsorption on hydrochar is complex or has multiple pathways. The general order equation shows different *n* (order of adsorption rate) values depending on the adsorbate concentration, which makes the comparison of different kinetic parameters of the model highly difficult (dos reis et al. 2022; dos Reis et al. 2021; Teixeira et al. 2021).

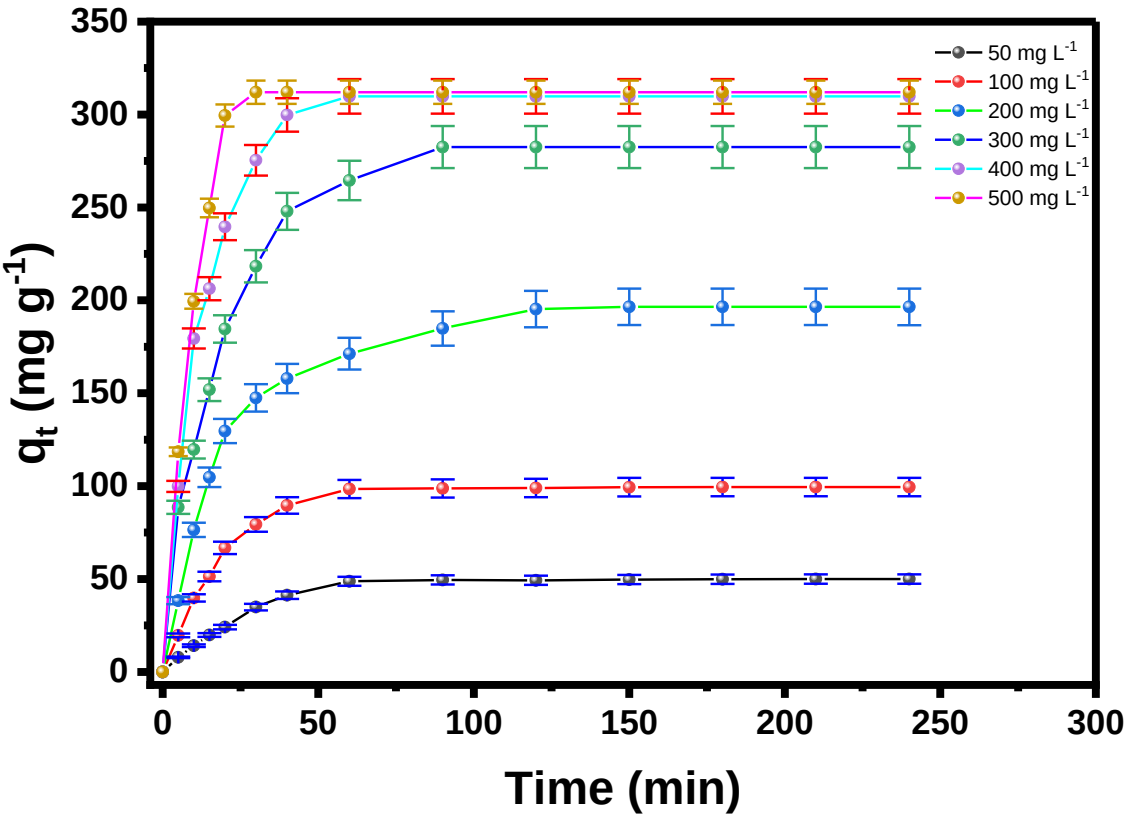

Fig. 4. Kinetic curves of Ce(III) adsorption onto hydrochar.

Notwithstanding, for increased understanding of the kinetic process, parameters such as $t_{1/2}$ and $t_{0.95}$ mean the time necessary to attain 50% ($t_{0.5}$) and 95% ($t_{0.95}$) of maximum adsorption capacity, respectively, were evaluated. It could be concluded that the time to reach 50% and 95% of the maximum capacity (q_e) of the hydrochar for Ce(III) were 19.7 and 71.6 min for 50 mg L^{-1}; 13.6 and 53.1 min for 100 mg L^{-1}; 13.9 and 88.4 min for 200 mg L^{-1}; 12.5 and 71.0 min for 300 mg L^{-1}; 8.6 and 41.0 min for 400 mg L^{-1}; and 6.7 and 27.1 min for 500 mg L^{-1}, respectively. These results show that most Ce(III) is adsorbed in the first hour regardless of the initial concentration, showcasing the high affinity between hydrochar and Ce(III).

Table 1. Kinetic parameters for Ce(III) adsorption onto hydrochar.

Model	Ce(III) initial concentration (mg L^{-1})					
	50	100	200	300	400	500
Pseudo-first order						
q_1 (mg g^{-1})	50.65	100.11	193.05	281.36	309.90	314.86
k_1 (min^{-1})	0.0371	0.0518	0.0490	0.0540	0.0776	0.1060
R^2_{adj}	0.9908	0.9969	0.9911	0.9930	0.9974	0.9916
SD (mg g^{-1})	1.65	1.78	5.80	7.18	4.64	8.29
Pseudo-second order						
q_2 (mg g^{-1})	58.20	111.10	215.90	310.00	334.00	334.00
k_2 (g mg^{-1} min^{-1})	0.00007489	0.0006149	0.0002929	0.0002412	0.0003537	0.0005322
R^2_{adj}	0.9661	0.9725	0.9911	0.9886	0.9801	0.9511
SD (mg g^{-1})	3.34	5.61	6.11	9.68	13.54	20.98
General order						
q_n (mg g^{-1})	50.33	99.77	198.50	285.20	310.60	314.50
k_n (min^{-1} (g mg^{-1})$^{n-1}$)	0.0560	0.0732	0.0089	0.0159	0.0564	0.1310
n (-)	0.881	0.916	1.346	1.235	1.061	0.960
R^2_{adj}	0.9942	0.9981	0.9954	0.9952	0.9976	0.9930
$t_{0.5}$ (hour)	19.7	13.6	13.9	12.5	8.6	6.7
$T_{0.95}$ (hour)	71.6	53.1	88.4	71.0	41.0	27.1
SD (mg g^{-1})	1.37	1.44	4.38	6.27	6.78	7.96

Isotherms and thermodynamics results for Ce(III) adsorption on the WWH

To further evaluate the relationship between Ce(III) and hydrochar, isotherms of adsorption were used. Three isotherm models, e.g., Langmuir, Freundlich, and Liu, were

used to assess the fitness of the experimental equilibrium adsorption process (Feitoza et al. 2022; Teixeira et al. 2021).

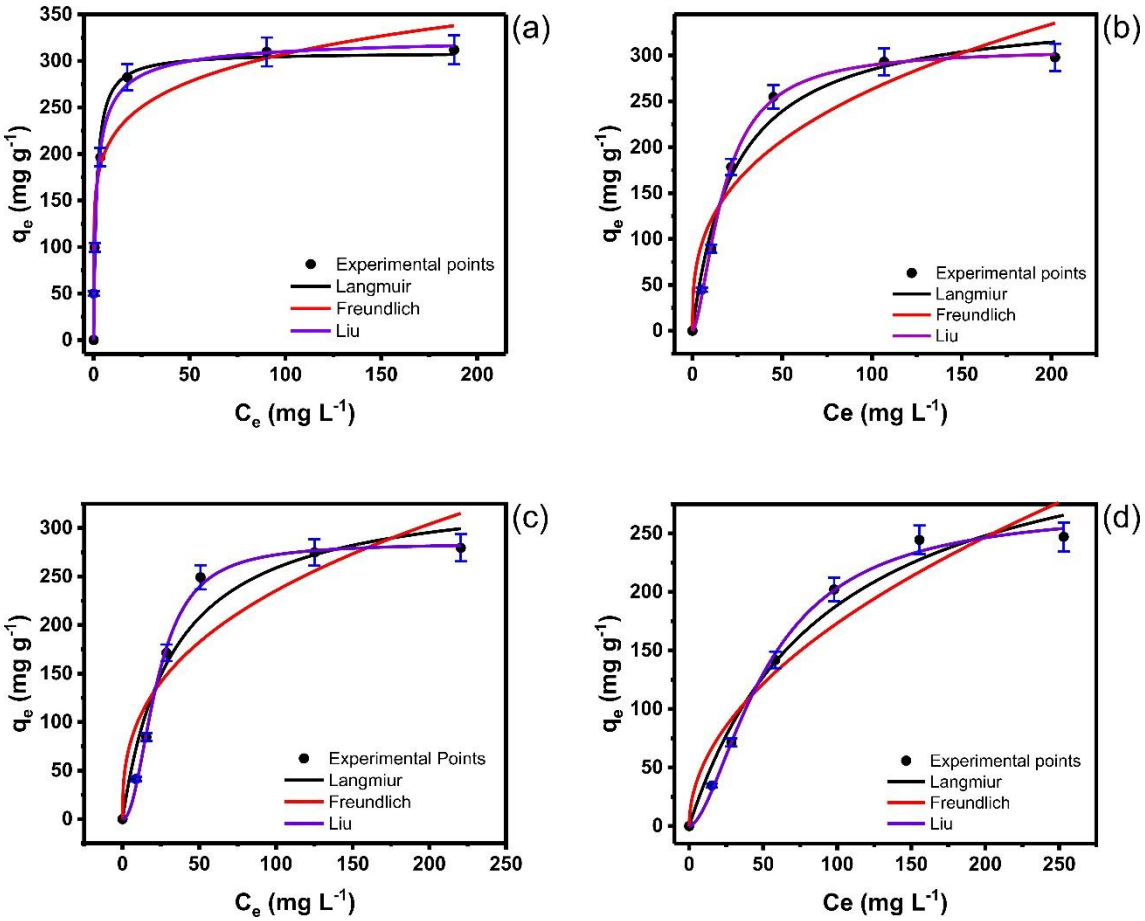

Fig. 5. Isotherms of Ce(III) adsorption on hydrochar at different temperatures; a) 298K, b) 308 K, c) 318 K, and d) 328 (adsorbent dosage of 1.0 g L^{-1}, pH of 6.0).

Furthermore, the isotherms were also evaluated at different temperatures varying from 298K to 328K (see Fig. 5). The curves show that with the temperature increase, the adsorption capacities decreased. However, even so, the hydrochar exhibited very high adsorption capacities suggesting a high affinity between hydrochar and cerium. Furthermore, the high hydrochar efficiency on cerium removal can be related to the large presence of functionalities on its surface, previously shown in FTIR analysis. A detailed explanation of the effect of temperature on Ce(III) uptake is further examined in the later

289 section, the thermodynamic studies. However, this section remains focused solely on the
290 equilibrium process.

291 **Table 2.** Isotherm parameters for Ce(III) adsorption onto hydrochar adsorbent.

	298K	308K	318K	328K
Langmuir				
Q_{max} (mg g^{-1})	309.4	351.3	344.1	362.2
K_L (L mg^{-1})	0.6601	0.0427	0.0356	0.0108
R^2_{adj}	0.9586	0.9771	0.9442	0.9732
SD (mg g^{-1})	26.40	18.50	27.42	16.55
Freundlich				
K_F (mg g^{-1} (mg $L^{-1})^{-1/nF}$)	155.3	53.7	43.0	16.5
n_F	6.734	2.899	2.711	1.961
R^2_{adj}	0.9170	0.8790	0.8429	0.9179
SD (mg g^{-1})	37.34	42.55	46.01	28.99
Liu				
Q_{max} (mg g^{-1})	327.9	307.1	284.3	272.2
K_g (L mg^{-1})	0.5737	0.0571	0.0441	0.0189
n_L	0.706	1.609	2.110	1.687
R^2_{adj}	0.9604	0.9986	0.9966	0.9951
SD (mg g^{-1})	25.78	4.64	6.72	7.09

292
293 Evaluating the suitability of the isotherm models, based on the same kinetic
294 parameters (R^2_{adj} and *SD)*, the Liu model was the most suitable because it presented the
295 highest R^2_{adj} and the lowest *SD*, showing the best fit to the experimental values.
296 Nevertheless, the Langmuir model presented R^2_{adj} and *SD* values close to Liu, suggesting
297 that Ce(III) uptake onto hydrochar displays some homogeneity in the process.

298 Table 3 reports the studies comparing the performance of various adsorbents for
299 cerium uptake. The data show that the q_{max} of Hydrochar is the highest among all
300 adsorbents presented in Table 3. However, the second highest q_{max} value was obtained
301 from *Sporopollenin* bio-hydrogel (278.2 m^2 g^{-1}), which makes its synthesis process more
302 complex and costs much higher than the hydrochar prepared in this work. Thus,
303 considering that the cost of the adsorbent fabrication is an important parameter to observe,

our hydrochar can be considered an effective adsorbent to adsorb Ce(III) from an aqueous solution.

Table 3. Comparison of the q_{max} for Ce(III) dye using different adsorbents.

Adsorbents	**q_{max} (mg g^{1})**	**pH**	**Reference**
Pinus brutia leaf powder	17.2	4.0	Kütahyali et al. (2010)
Modified Pinus brutia leaf powder	62.1	6.0	Kütahyali et al. (2012)
Multi-walled carbon nanotubes	92.59	5.0	Behdani et al. (2013)
Xylan bio-hydrogel	180.4	6.0	Varsihini et al. (2015)
Sporopollenin bio-hydrogel	278.2	6.0	Varsihini et al. (2015)
Poly (allylamine)/silica composite	111.8	5.0	Zhou et al. (2015)
EDTA-cross-linked -cyclodextrin biopolymer	49.42	4.0	Zhao et al. (2016)
Chitosan/Polyvinyl alcohol/3-mercaptopropyltrimethoxysilane	251.4	6.0	Najafi Lahiji et al. (2016)
Zn/Al Layered double hydroxide intercalated cellulose	96.25	5.0	Iftekhar et al. (2017)
Hydrochar	327.9	6.0	This work

Table 4 depicts the thermodynamic adsorption data for Ce(III) onto hydrochar adsorbent.

Table 4. Thermodynamic parameters of Ce(III) on hydrochar material.

T (K)	K (-)	ΔG^0 (kJ mol^{-1})	ΔH^0 (kJ mol^{-1})	ΔS^0 (kJ mol^{-1} K^{-1})
298	80384.5	-27.98		
308	8000.6	-23.01	-86.02	0.198
318	6179.1	-23.08		
328	2648.2	-21.50		

As can be seen, the K parameter is reduced as the temperature increases, indicating that the adsorption of Ce(III) onto the hydrochar was not favored at high temperatures. However, according to the thermodynamic equilibrium data, the adsorption process was spontaneous and favorable (298-328 K), with a value of $\Delta G° < 0$. Furthermore, the adsorption process was exothermic ($\Delta H° < 0$) (Lima et al. 2020). In addition, the enthalpy values are compatible with electrostatic attraction or chelation. Therefore these are the

major Ce(III) mechanisms of interaction with our hydrochar, although other mechanisms could be involved in minor importance (Chang and Thoman-Jr 2014; Lima et al. 2021a). Finally, the $\Delta S° > 0$ indicates that Ce(III) was adsorbed at disorganized sites, possibly due to the different surface functionalities (Lima et al. 2021).

Ce(III) desorption studies and reusability of hydrochar

As discussed earlier in this paper, the solution pH significantly affects Ce(III) uptake with a largely reduced capacity at acidic pH; hence, the desorption process of Ce(III) was performed by varying the solution of H_2SO_4 from 0.1 to 5 mol L^{-1}. In addition, the Ce(III)-loaded hydrochar was subjected to desorption tests to examine the degree of recovery of Ce(III) and the potential reusability of hydrochar, making the process even more sustainable and cheaper.

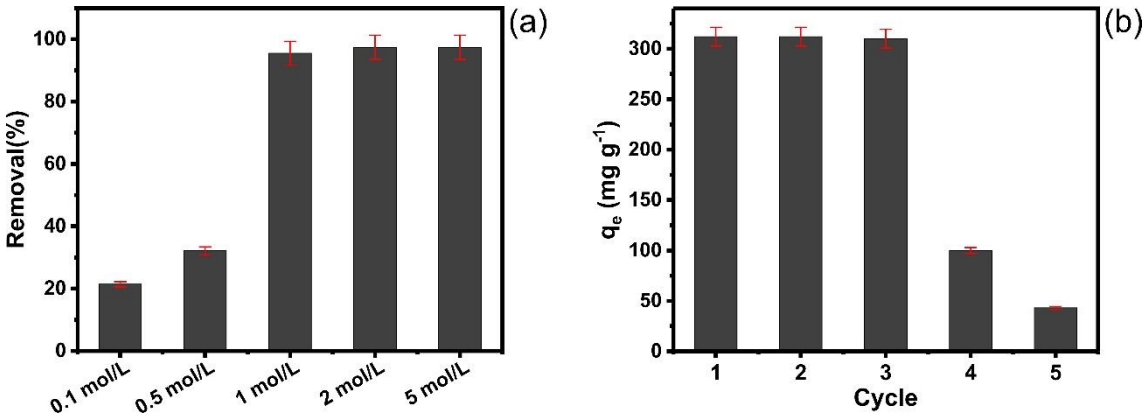

Fig. 6. Desorption tests under different acid concentration solutions (a) and reusability tests for 5 cycles (b).

The desorption tests were conducted at 25 °C using a Ce(III)-loaded hydrochar (312 mg g^{-1}) and a total mass (hydrochar+Ce(III)) of 3.0g in an eluent volume of 100 mL. The desorption tests were stirred for 1 hour. The results showed that the lower H_2SO_4

concentrations, 0.1 and 0.5 mol L^{-1} were insufficient to desorb the Ce(III) from hydrochar structure (See Fig.6a). However, at higher concentrations (>1.0 mol L^{-1}), the Ce(III) was almost completely desorbed reaching a value of 95.5%, showing to be an extremely efficient approach (see Fig.6a).

The adsorbed Cerium extraction from hydrochar structure might be governed by a cation-exchange mechanism which implies that for the desorption process (Gaete et al. 2021), it is necessary to change the chemical equilibrium by using a strong acid agent (H_2SO_4), which liberates of Ce(III) in the aqueous phase, for easy recovery. Since the difference between desorption percentages was smaller than 2% between 1, 2, and 5 mol L^{-1}, this first one was chosen to study the cyclability tests because it would reduce the costs of the process using lower acid solution concentration. The hydrochar loaded with Ce(III) was subjected to six adsorption-desorption cycles, and the results demonstrated that until the third cycle, the adsorption capacity was almost constant (nearly 100%) and suffered an extreme reduction in the fourth cycle (see Fig.6b).

Hydrochar as an adsorbent is already a sustainable and efficient approach for water decontamination, and the reusability in several cycles, as demonstrated in this work, further improves the sustainability and environmental friendliness of the application.

Mechanism of Ce(III) adsorption

Based on the results of the characterization of hydrochar and the kinetics, equilibrium, thermodynamic, and desorption data, a possible mechanism of adsorption is proposed (See Fig. 7). Electrostatic interaction was found to be an important adsorption mechanism ruling Ce(III) and hydrochar's surface interactions due to the attraction of positively charged Ce(III) to the hydrochar's surface. At the same time, other interactions also took place, such as surface precipitation that may occur between Ce(III) and some anionic

groups on the hydrochar surface (e.g., OH and COOH). For the surface complexation, the hydroxyl groups on the adsorbent surface interact with Ce(III), subsequently leading to surface complexation (Huang et al. 2021; Li et al. 2021).

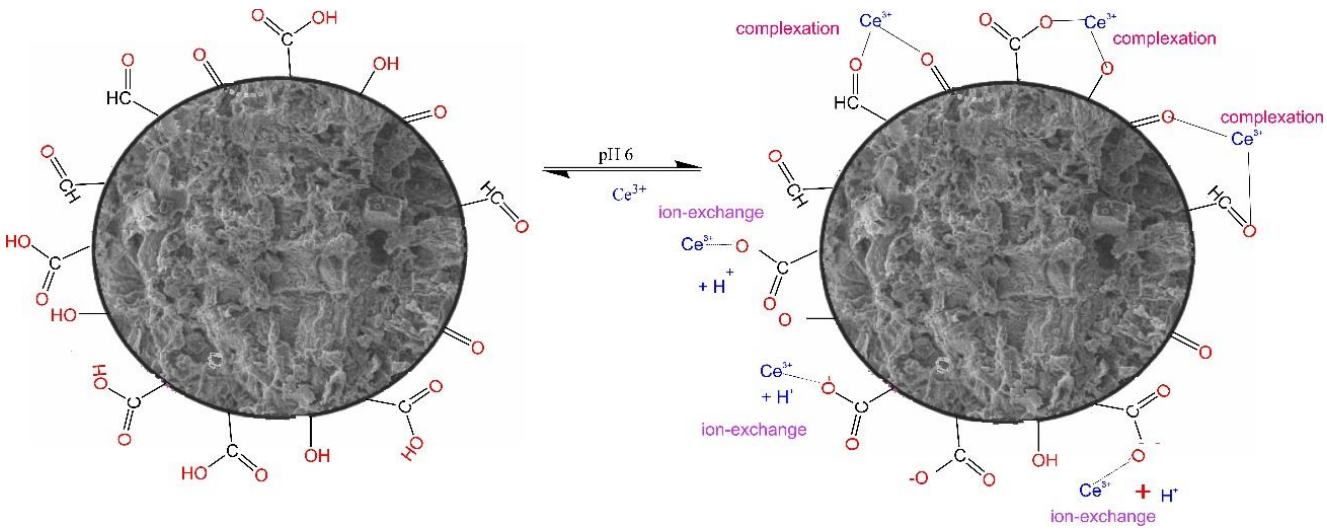

Fig. 7. Main Ce(III) adsorption mechanism onto hydrochar surface.

A hydrochar surface rich in oxygen-containing groups (e.g., OH and COOH) promote surface reactions, and complexation may have an important role in the Ce(III) uptaken due to the amphoteric behavior of hydroxyl groups (Huang et al. 2021). Also, the abundant oxygen-containing groups on the hydrochar surface are conducive to attracting and adsorbing Ce(III) through surface complexes and precipitates. The hydrochar regions of π-electrons, lone pair electrons, and electron donors in aliphatic C-, C=C, aromatic C=O, and alkane groups are also likely to interact with Ce(III) (Li et al. 2021). Zhu et al. (2020) reported that functionalities such as C-H and C=O play an important role in heavy metal adsorption through π-bonding.

Results of the real wastewater treatment

The results of Ce uptake from the real wastewater using the hydrochar are depicted in Fig. 8. As we can see, the hydrochar dosage increase caused an increase in the Ce uptake

from the effluent. Hydrochar dosages until 4 g L^{-1} provided maximum uptakes of 20%. Also, dosages until 7 g L^{-1} provided uptake until 60%. These poor results could be explained by the complex features of the wastewater, which contains several rare earths, phosphates, carbonates, calcium, and iron. On the other hand, using 8 g L^{-1} of the hydrochar provided a Ce uptake of 86%. So, the hydrochar proved efficient in treating real wastewater containing a complex composition.

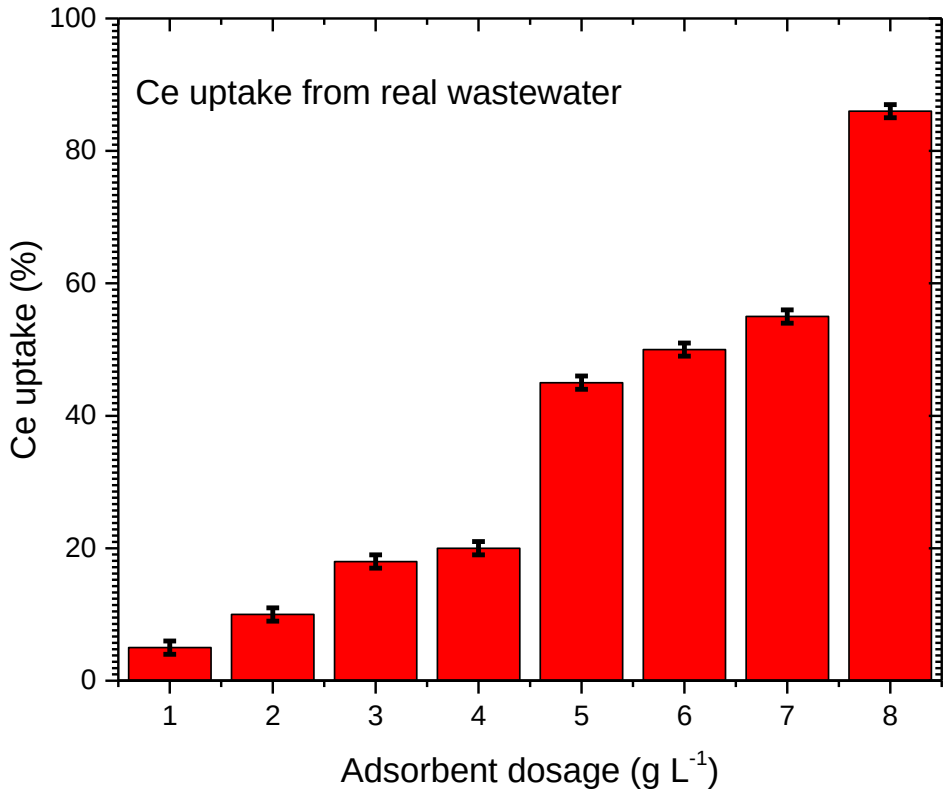

Fig. 8. Ce uptake from the real wastewater using different adsorbent dosages (200 rpm, 240 min, 298 K).

Conclusion

Natural biomass material was subjected to HTC treatment to produce a sustainable hydrochar adsorbent for rare earth element Ce(III) adsorption and recovery. The hydrochar exhibited a very low BET surface area (8.8 $m^2\ g^{-1}$) but was extremely rich in functional groups on its surface. Assays of the effect of the initial pH on Ce(III) removal indicated that the highest Ce(III) removal was obtained at pH 6.0. The kinetics and equilibrium data showed the best fit using the General order and Liu equilibrium model, respectively. The adsorption capacity of hydrochar for Ce(III) reached 327.9 $mg\ g^{-1}$, higher than many reported adsorbents. The thermodynamic parameters for Ce(III) removal were obtained based on the Liu equilibrium data. The Ce(III) removal using our hydrochar was favorable and spontaneous ($\Delta G°<0$) (~ -21.50 to -27.08 kJ mol^{-1}), and exothermic ($\Delta H°<0$), indicating that electrostatic attraction was the main mechanism as well with surface complexation and ion exchange. The desorption tests indicated that a 1 mol L^{-1} H_2SO_4 was enough to desorb nearly 100% of the adsorbed Ce(III). The reusability tests proved that the hydrochar could be used three times without losing adsorptive performance. Finally, the material efficiently treated a real wastewater sample reaching a Ce uptake of 86%. Hydrochar as an adsorbent is already a sustainable and efficient material for adsorbing ions, but the ability to use it several times makes the technology much more sustainable and environmentally friendly.

Acknowledgments

This work was funded by Brazilian National Council for Scientific and Technological Development/CNPq (Grants 405982/2022-4, 303992/2021-2, 303.612/2021-5, and 402.450/2021-3) and Coordination for the Improvement of Higher Education Personnel/CAPES (CAPES-Print program). Dr. dos Reis thanks Bio4Energy - a Strategic

Research Environment appointed by the Swedish government and the Swedish University of Agricultural Sciences, for the funding support.

References

Ahmed Amine Azzaz, Besma Khiari, Salah Jellali, Camélia Matei Ghimbeu, Mejdi Jeguirim, Hydrochars production, characterization and application for wastewater treatment: A review, Renewable and Sustainable Energy Reviews 127, 2020, 109882. https://doi.org/10.1016/j.rser.2020.109882,

Balaram V, (2019) Rare earth elements: A review of applications, occurrence, exploration, analysis, recycling, and environmental impact, Geoscience Frontiers 10: 1285-1303. https://doi.org/10.1016/j.gsf.2018.12.005

Behdani FN, Rafsanjani AT, Torab-Mostaedi M, Mohammadpour SMAK (2013). Adsorption ability of oxidized multi-walled carbon nanotubes towards aqueous Ce(III) and Sm(III). Korean J Chem Eng 30:448–455. https://doi.org/10.1007/s11814-012-0126-9

Bhatnagar, A., Kaczala, F., Hogland, W. et al. Valorization of solid waste products from the olive oil industry as potential adsorbents for water pollution control—a review. Environ Sci Pollut Res 21, 268–298 (2014). https://doi.org/10.1007/s11356-013-2135-6

Cimirro, N.F.G.M., Lima, E.C., Cunha, M.R., Thue, P.S., Grimm, A., dos Reis, G.S., Rabiee, N., Saeb, M.R., Keivanimehr, F., Habibzadeh, S. (2022). Removal of diphenols using pine biochar. Kinetics, equilibrium, thermodynamics, and mechanism of uptake. Journal of Molecular Liquids, 364, 119979. Doi:10.1016/j.molliq.2022.119979.

Cunha, M.R., Lima, E.C., Lima, D.R., da Silva, R.S., Thue, P.S., Seliem, M.K., Sher, F., dos Reis, G.S., Larsson, S.H. (2020) Removal of captopril pharmaceutical from synthetic pharmaceutical-industry wastewaters: use of activated carbon derived from *Butia catarinensis*. J Environ Chem Eng, 8,1–9. DOI: 10.1016/j.jece.2020.104506.

dos Reis GS, Guy M, Mathieu M, Jebrane M, Lima EC, Thyrel M, Dotto GL, Larsson SH (2022b) A comparative study of chemical treatment by $MgCl_2$, $ZnSO_4$, $ZnCl_2$, and KOH on physicochemical properties and acetaminophen adsorption performance of biobased porous materials from tree bark residues. Colloids Surf a: Physicochem Eng Aspects 642:1–13. https://doi.org/10.1016/j.colsurfa.2022.128626

dos Reis, G. S., Pinto, D., Lima, É. C., Knani, S., Grimm, A., Silva, L. F., Cadaval, T. R., & Dotto, G. L. (2022c). Lanthanum uptake from water using chitosan with different configurations. Reactive and Functional Polymers, 180, 105395. https://doi.org/10.1016/j.reactfunctpolym.2022.105395

Dos Reis, G.S., Larsson, S.H., Mathieu, M., Thyrel, M., Tung, P., (2021a). Application of Design of Experiments (DoE) for Optimised Production of Micro-and Mesoporous Norway Spruce Bark Activated Carbons. Biomass Conv. Bioref. https://doi.org/10.1007/s13399-021-01917-9

Dos Reis, G.S., Oliveira, H.P.d., Larsson, S.H., Thyrel, M., Lima, E.C., (2021b). A short review on the electrochemical performance of hierarchical and nitrogen-doped activated biocarbon-based electrodes for supercapacitors. Nanomaterials 11, 424. https://doi.org/10.3390/nano11020424.

Feitoza, U.S., Thue, P.S., Lima, E.C., dos Reis, G.S., Rabiee, N., de Alencar, W.S., Mello, B.L., Dehmani, Y., Rinklebe, J., Dias, S.L.P. (2022). Use of Biochar Prepared from the Açaí Seed as Adsorbent for the Uptake of Catechol from Synthetic Effluents.

Molecules 27, 7570. Doi:10.3390/molecules27217570.

Feng, Y., Sun, H., Han, L., Xue, L., Chen, Y., Yang, L., & Xing, B. (2019). Fabrication of hydrochar based on food waste (FWHTC) and its application in aqueous solution rare earth ions adsorptive removal: Process, mechanisms and disposal methodology. Journal of Cleaner Production, 212, 1423-1433. https://doi.org/10.1016/j.jclepro.2018.12.094

Fernandez, V. (2017). Rare-earth elements market: A historical and financial perspective. Resources Policy, 53, 26-45. https://doi.org/10.1016/j.resourpol.2017.05.010

Gaete J. Molina L. Valenzuela F. Basualto C (2021). Recovery of lanthanum, praseodymium, and samarium by adsorption using magnetic nanoparticles functionalized with a phosphonic group, Hydrometallurgy 203 (2021) 105698. https://doi.org/10.1016/j.hydromet.2021.105698

Georgin J, Franco DSP, Grassi P, Tonato D, Piccilli DGA, Meili L, Dotto GL (2019) Potential of Cedrella fissilis bark as an adsorbent for the removal of red 97 dye from aqueous effluents. Environ Sci Pollut Res 26:19207–19219. https://doi.org/10.1007/s11356-019-05321-9

Georgin J, Franco DSP, Netto MS, Allasia D, Oliveira MLS, Dotto GL (2020) Treatment of water containing methylene by biosorption using Brazilian berry seeds (Eugenia uniflora). Environ Sci Pollut Res 27:20831–20843. https://doi.org/10.1007/s11356-020-08496-8

Gonzalez-Hourcade M, G. Simoes ˜ dos Reis, A. Grimm, V.M. Dinh, E.C. Lima, S. H. Larsson, F.G. Gentili, Microalgae biomass as a sustainable precursor to produce nitrogen-doped biochar for efficient removal of emerging pollutants from aqueous media, J. Clean. Prod. 348 (2022), 131280, https://doi.org/10.1016/j. jclepro.2022.131280

GS dos Reis, CM Subramaniyam, AD Cárdenas, SH. Larsson, M Thyrel, Ulla Lassi, F García-Alvarado (2022a). Facile Synthesis of Sustainable Activated Biochars with Different Pore Structures as Efficient Additive-Carbon-Free Anodes for Lithium- and Sodium-Ion Batteries, ACS Omega 7, 42570−42581. https://doi.org/10.1021/acsomega.2c06054

Guy M, Mathieu M, Anastopoulos IP, Martínez MG, Rousseau F, Dotto GL, de Oliveira HP, Lima EC, Thyrel M, Larsson SH, dos Reis GS (2022) Process parameters optimization, characterization, and application of KOH-activated Norway spruce bark graphitic biochars for efficient azo dye adsorption. Molecules 27:1–25. https://doi.org/10.3390/molecules27020456

Huang T, Zhang S-W, Xie J, Zhou L, Liu L-F (2021) Effective adsorption of quadrivalent cerium by synthesized lauryl sulfonate green rust in a central composite design, journal of environmental sciences 107; 14–25

Iftekhar S, Srivastava V, Sillanpää M (2017) Synthesis and application of LDH intercalated cellulose nanocomposite for separation of rare earth elements (REEs). Chem Eng J 309:130–139. https://doi.org/10.1016/j.cej.2016.10.028

Jiang, L., Sheng, L. & Fan, Z. Biomass-derived carbon materials with structural diversities and their applications in energy storage. Sci. China Mater. 61, 133–158 (2018). https://doi.org/10.1007/s40843-017-9169-4

Kabir MM, Akter MM, Khandaker S, Gilroyed BH, Didar-ul-Alam M, Hakim M, Awual MR (2022a) Highly effective agro-waste based functional green adsorbents for toxic chromium(VI) ion removal from wastewater. J Mol Liq 347:118327. https://doi.org/10.1016/j.molliq.2021.118327

Kabir MM, Alam F, Akter MM, Gilroyed BH, Didar-ul-Alam M, Tijing L, Shon HK (2022b) Highly effective water hyacinth (Eichhornia crassipes) waste-based

519 functionalized sustainable green adsorbents for antibiotic remediation from
520 wastewater. Chemosphere 304:135293.
521 https://doi.org/10.1016/j.chemosphere.2022.135293
522 Kabir MM, Ferdousi S, Rahman MM, Uddin MK (2019) Chromium (VI) removal
523 efficacy from aqueous solution by modified tea wastes-polyvinyl alcohol (TW-
524 PVA) composite adsorbent. Desalination Water Treat 174:311–323.
525 Kabir MM, Mouna SSP, Akter S, Khandaker S, Didar-ul-Alam M, Bahadur NM,
526 Mohinuzzaman M, Islam MA, Shenashen MA (2021) Tea waste based natural
527 adsorbent for toxic pollutant removal from waste samples. J Mol Liq 322:115012.
528 https://doi.org/10.1016/j.molliq.2020.115012
529 Keiluweit, M., Nico, P. S., Johnson, M. G., and Kleber, M. (2010). Dynamic molecular
530 structure of plant biomass-derived black carbon (biochar), Environ. Sci. Technol.
531 44, 1247-1253. DOI: 10.1021/es9031419
532 Khoshbouy, R., Takahashi, F., & Yoshikawa, K. (2019). Preparation of high surface area
533 sludge-based activated hydrochar via hydrothermal carbonization and application
534 in the removal of basic dye. Environmental Research, 175, 457-467.
535 https://doi.org/10.1016/j.envres.2019.04.002
536 Kütahyali C, Sert S, Cetinkaya B, Inan S, Eral M (2010) Factors affecting lanthanum and
537 cerium biosorption on Pinus brutia leaf powder. Sep Sci Technol 45:1456–1462.
538 https://doi.org/10.1080/01496391003674266
539 Kütahyali C, Sert S, Cetinkaya B, Yalcintas E, Acar MB (2012) Biosorption of Ce(III)
540 onto modified Pinus brutia leaf powder using central composite design. Wood Sci
541 Technol 46:721–736. https://doi.org/10.1007/s00226-011-0437-8
542 Li D, Cui H, Cheng Y, Xue L, Wang B, He H, Hua Y, Chu Q, Feng Y, Yang L (2021)
543 Chemical aging of hydrochar improves the Cd2+ adsorption capacity from aqueous

544 solution, Environmental Pollution 287; 117562
545 Li, B., Liu, JL. & Xu, H. (2022) Synthesis of polyaminophosphonated-functionalized
546 hydrochar for efficient sorption of Pb(II). Environ Sci Pollut Res 29, 49808–49815.
547 https://doi.org/10.1007/s11356-022-19350-4
548 Lima EC, Naushad M, dos Reis GS, Dotto GL, Pavan FA, Guleria A, Seliem MK, Sher
549 F, (2022a). Production of carbon-based adsorbents from lignocellulosic biomass. In
550 Biomass-Derived Materials for Environmental Applications; Anastopoulos, I.,
551 Lima, E.C., Meili, L., Giannakoudakis, D.A., Eds.; Elsevier: Amsterdam, The
552 Netherlands, 2022; pp. 169–191. ISBN 978-0-323-91914-2.
553 Lima ÉC, Pinto D, Schadeck Netto M, Dos Reis GS, Silva LFO, Dotto GL. (2022b)
554 Biosorption of Neodymium (Nd) from Aqueous Solutions Using *Spirulina*
555 *platensis* sp. Strains. *Polymers*. 2022; 14(21):4585.
556 https://doi.org/10.3390/polym14214585
557 Lütke SF, Oliveira MLS, Waechter SR, Silva LFO, Cadaval Jr. TRS, Duarte FA, Dotto
558 GL (2022) Leaching of rare earth elements from phosphogypsum. Chemosphere
559 301:134661. https://doi.or/10.1016/j.chemosphere.2022.134661.
560 Najafi Lahiji M, Keshtkar AR, Moosavian MA (2018) Adsorption of cerium and
561 lanthanum from aqueous solutions by chitosan/polyvinyl alcohol/3-
562 mercaptopropyltrimethoxysilane beads in batch and fixed-bed systems. Part Sci
563 Technol 36:340-350. https://doi.org/10.1080/02726351.2016.1248262
564 Netto MS, Georgin J, Franco DSP, et al. (2022) Effective adsorptive removal of atrazine
565 herbicide in river waters by a novel hydrochar derived from Prunus serrulata bark.
566 Environ Sci Pollut Res 29, 3672–3685. https://doi.org/10.1007/s11356-021-15366-
567 4
568 Taelman, S.E.; Tonini, D.; Wandl, A.; Dewulf, J. A Holistic Sustainability Framework

for Waste Management in European Cities: Concept Development. Sustainability 2018, 10, 2184. https://doi.org/10.3390/su10072184

Teixeira, R.A., Lima, E.C., Benetti, A.D., Thue, P.S., Cunha, M.R., Cimirro, N.F.G.M., Sher, F., Dehghani, M.H., dos Reis, G.S., Dotto, G.L. (2021) Preparation of hybrids of wood sawdust with 3-aminopropyltriethoxysilane. Application as an adsorbent to remove Reactive Blue 4 dye from wastewater effluents. J. Taiwan Inst. Chem. Eng. 125, 141-152. Doi:10.1016/j.jtice.2021.06.007

Varsihini C, Das JS, Das DN (2015) Recovery of cerium (III) from electronic industry effluent using novel biohydrogel: batch and column studies. Der Pharmacia Lettre 7: 166–179

Wang T, Zhai Y, Zhu Y, Li C, Zeng G (2018) A review of the hydrothermal carbonization of biomass waste for hydrochar formation: process conditions, fundamentals, and physicochemical properties. Renew Sust Energ Rev 90:223–247. https://doi.org/10.1016/j.rser. 2018.03.071

Xiao K, Liu H, Li Y, Yang G, Wang Y, Yao H (2020) Excellent performance of porous carbon from urea-assisted hydrochar of orange peel for toluene and iodine adsorption. Chem Eng J 382:122997. https://doi.org/10.1016/j.cej.2019.122997

Yamil YL, Georgin J, dos Reis GS et al. (2020) Utilization of Pacara Earpod tree (Enterolobium contortisilquum) and Ironwood (Caesalpinia leiostachya) seeds as low-cost biosorbents for removal of basic fuchsin. Environ Sci Pollut Res 27:33307–33320. https://doi.org/10.1007/s11356-020-09471-z

Yan W, Zhang H, Sheng K, Mustafa AM, Yu Y (2018) Evaluation of engineered hydrochar from KMnO4 treated bamboo residues: physicochemical properties, hygroscopic dynamics, and morphology. Bioresour Technol 250:806–811. https://doi.org/10.1016/j.biortech.2017.11.052

Zhao F, Repo E, Meng Y, Wang X, Yin D, Sillanpää M (2016) An EDTA- -cyclodextrin material for the adsorption of rare earth elements and its application in preconcentration of rare earth elements in seawater. J Colloid Interface Sci 465: 215–224.

Zhou S, Li X, Shi Y, Alshameri A, Yan C (2015) Preparation, characterization, and Ce(III) adsorption performance of poly(allylamine)/silica composite. Desalin. Water Treat 56:1321–1334. https://doi.org/10.1080/19443994.2014.944221

Declarations

-Authors Contributions

Conceptualization: [Glaydson S. dos Reis, Julien Vieillard, Guilherme L. Dotto]; Methodology: [Carlos E. Schnoor, Matias S. Netto], Formal analysis and investigation: [Eder C. Lima, Irineu A.S. de Brum]; Writing - original draft preparation: [Mykel Thyrel,

Glaydson S. dos Reis, Ulla Lassi, Guilherme L. Dotto]; Writing - review and editing: [Glaydson S. dos Reis, Eder C. Lima, Luis F.O. Silva, Guilherme L. Dotto]; Funding acquisition: [Guilherme L. Dotto, Luis F.O. Silva]; Supervision: [Luis F.O. Silva, Guilherme L. Dotto]. All authors read and approved the final manuscript.

-Ethical Approval

Not applicable.

-Consent to Participate

Not applicable.

-Consent to Publish

Not applicable.

-Competing Interests

The authors declare that they have no competing interests.

-Availability of data and materials

The datasets used and analyzed during the current study are available from the corresponding author upon reasonable request.